Cell Host & Microbe
Article

Two Mosquito LRR Proteins Function as Complement Control Factors in the TEP1-Mediated Killing of *Plasmodium*

Malou Fraiture,[1,4] Richard H.G. Baxter,[2,3,4] Stefanie Steinert,[1] Yogarany Chelliah,[2,3] Cécile Frolet,[1,5] Wilber Quispe-Tintaya,[1,6] Jules A. Hoffmann,[1] Stéphanie A. Blandin,[1] and Elena A. Levashina[1,*]
[1]UPR 9022 CNRS, AVENIR group Inserm, Institut de Biologie Moléculaire et Cellulaire (IBMC), 15 rue René Descartes, 67084 Strasbourg, France
[2]Department of Biochemistry
[3]Howard Hughes Medical Institute
University of Texas Southwestern Medical Center, 6001 Forest Park Road, Dallas, TX 75390-9050, USA
[4]These authors contributed equally to this work
[5]Present address: UMR 5075 CEA/CNRS/UJF, Institut de Biologie Structurale Jean-Pierre Ebel (IBS), Laboratoire d'Ingénierie des Macromolécules, 41 rue Jules Horowitz, 38027 Grenoble, France
[6]Present address: Department of Microbiology and Immunology, Albert Einstein College of Medicine, 1300 Morris Park Avenue, Bronx, NY 10461, USA
*Correspondence: e.levashina@ibmc.u-strasbg.fr
DOI 10.1016/j.chom.2009.01.005

SUMMARY

Plasmodium **development within *Anopheles* mosquitoes is a vulnerable step in the parasite transmission cycle, and targeting this step represents a promising strategy for malaria control. The thioester-containing complement-like protein TEP1 and two leucine-rich repeat (LRR) proteins, LRIM1 and APL1, have been identified as major mosquito factors that regulate parasite loads. Here, we show that LRIM1 and APL1 are required for binding of TEP1 to parasites. RNAi silencing of the LRR-encoding genes results in deposition of TEP1 on *Anopheles* tissues, thereby depleting TEP1 from circulation in the hemolymph and impeding its binding to *Plasmodium*. LRIM1 and APL1 not only stabilize circulating TEP1, they also stabilize each other prior to their interaction with TEP1. Our results indicate that three major antiparasitic factors in mosquitoes jointly function as a complement-like system in parasite killing, and they reveal a role for LRR proteins as complement control factors.**

INTRODUCTION

Protozoan parasites of the *Plasmodium* genus persist and amplify in vertebrate hosts during their asexual stage and depend on mosquitoes for completion of their sexual cycle and further transmission. Mosquitoes ingest gametocytes by taking a blood meal on an infected vertebrate. After fertilization of male and female gametes, the zygotes differentiate into motile ookinetes that traverse the midgut epithelium to reach the basal side. There they develop into oocysts that undergo multiple rounds of cellular divisions, forming numerous sporozoites. Mature oocysts rupture and release the sporozoites into the hemolymph, the mosquito blood. Sporozoites migrate from the midgut to the salivary glands and are transmitted to a new host during the next mosquito bite (Sinden, 2002).

The development of *Plasmodium* in the mosquito is considerably hindered by a powerful insect immune response. Major parasite losses occur at the ookinete stage after its passage through the midgut epithelium within the first 24 hr postinfection (hpi) (Whitten et al., 2006). This antiparasitic defense has been mostly analyzed in laboratory conditions with the rodent malaria *Plasmodium berghei* as a model (Janse and Waters, 1995). Recent reverse genetics studies identified several genes encoding secreted proteins that crucially determine the outcome of *P. berghei* development in *Anopheles gambiae*. Among them is the complement-like glycoprotein TEP1 (Blandin et al., 2008).

TEP1 belongs to the family of thioester-containing proteins that share sequence similarity with the vertebrate complement factors C3/C4/C5 and α_2-macroglobulins (Blandin and Levashina, 2004). The vertebrate complement system comprises around 35 serum and cell-surface molecules that interact in a cascade, ultimately resulting in opsonization of pathogens and in induction of inflammatory responses at the site of infection. It is triggered by recognition and binding of a series of circulating factors to pathogen surfaces. These factors include antibodies, mannan-binding lectins, and ficolins. The alternative pathway does not require an initial recognition event and is constitutively activated by a low-level hydrolysis of the complement factor C3 and its association with factor B. All pathways trigger proteolytic cascades that converge upon the massive activation of the central component C3 and generation of its cleavage products that fulfill the major functions of the complement system: (1) binding of the larger proteolytic fragment C3b to microbes initiates the assembly of the membrane attack complex, which forms a pore in pathogen membranes and causes their lysis; (2) further cleavage of C3b produces iC3b that interacts with complement receptors and thus promotes

phagocytosis of opsonized microbes; (3) a cleavage product of iC3b, C3d, is recognized by another class of complement receptors that activate B lymphocytes; and finally, (4) soluble anaphylatoxins C3a, C4a, and C5a, clipped off from the α chains of the corresponding complement factors, cause inflammation and recruitment of immune cells at the site of complement activation (Lambris et al., 1999).

In *A. gambiae*, TEP1 is constitutively produced by hemocytes, the mosquito blood cells, and is secreted into the hemolymph as a full-length form (TEP1-F) of 160 kDa. Here, it is processed into an ~75 kDa N-terminal (TEP1-N) and an ~85 kDa C-terminal fragment (TEP1-C), containing the thioester bond. The three-dimensional structure of TEP1 reveals a close structural homology between TEP1 and the human complement factor C3 (Baxter et al., 2007) and predicts that, like in C3, the two chains of cleaved TEP1 should remain associated, forming a single complex due to the interdigitation of their secondary structure elements.

Similar to complement factors, TEP1 binds to the surface of Gram-negative and Gram-positive bacteria. Inactivation of the thioester by methylamine treatment abolishes binding of TEP1-C and delays phagocytosis of bacteria. This is in sharp contrast to the full-length TEP1, which binds bacteria in a thioester-independent manner but is unable to promote uptake of bacteria (Levashina et al., 2001). In adult mosquitoes, knockdown of *TEP1* dramatically impairs phagocytosis of *Escherichia coli* and *Staphylococcus aureus*, and therefore TEP1 plays a very similar role to C3 (Moita et al., 2005).

As is the case for bacteria, TEP1 is detected on the surface of invading ookinetes by immunofluorescence analysis of *P. berghei*-infected midguts using antibodies directed against TEP1-C. Furthermore, knockdown of *TEP1* by injection of specific dsRNA into the mosquitoes increases by 3- to 5-fold the burden of developing oocysts (Blandin et al., 2004). TEP1 also mediates killing of the most deadly human malaria parasite, *P. falciparum* (Dong et al., 2006), demonstrating that parasite elimination by the complement-like protein is a conserved component of the mosquito immune responses against rodent and human plasmodia. *TEP1* gene is exceptionally polymorphic, especially in the thioester domain and in the regions surrounding it. Two highly divergent alleles, *TEP1s* and *TEP1r*, were identified in laboratory-selected susceptible and refractory mosquito lines, respectively (Blandin et al., 2004; Collins et al., 1986). Recent evolutionary studies performed on mosquitoes collected in three sites in Africa suggest that these alleles resulted from a series of gene conversion events involving *TEP5* and *TEP6* genes, which are clustered with *TEP1* on the left arm of the third chromosome (Christophides et al., 2002; Obbard et al., 2008). To elucidate how *TEP1* polymorphism modulates the efficiency of parasite killing in the refractory line requires a better understanding of the sequence of molecular events, starting with TEP1 activation and binding to *Plasmodium* and leading to parasite killing. We postulated that activity of TEP1 is regulated by partner molecules and set out to identify them.

In addition to TEP1, two leucine-rich repeat (LRR) proteins, LRIM1 (leucine-rich repeat immune protein 1) and APL1 (*Anopheles Plasmodium*-responsive leucine-rich repeat 1), have been shown to strongly affect *P. berghei* development on the mosquito midgut (Blandin et al., 2004; Osta et al., 2004; Riehle et al., 2006). Their potency in the antiparasitic response is illustrated by the increase in parasite survival following knockdown by RNAi of the respective genes. *APL1* maps to the locus that controls resistance to human malaria parasites in African mosquito populations and is believed to be one of the major resistance factors in natural infections (Niare et al., 2002; Riehle et al., 2007). LRR proteins are involved in protein-protein interactions (Kobe and Kajava, 2001), and their important roles in innate immunity are well documented in plants and mammals (Nurnberger et al., 2004). In *P. berghei* infections, the knockdown phenotypes of *LRIM1* and *APL1* are very similar to that of *TEP1*: on average, all three result in a 3-fold increase in parasite loads in the mosquito midgut. Moreover, the expression of *TEP1* and *LRIM1* is regulated by the Cactus/Rel1 signaling cassette, further supporting the hypothesis that these genes might function in the same pathway (Frolet et al., 2006). We therefore investigated molecular interactions between TEP1, LRIM1, and APL1 using functional, cell biology, and immunobiochemical approaches.

Here, we report that proteolytic cleavage of TEP1 in the hemolymph is crucial for its maturation into a form that is maintained in circulation by a multiprotein complex involving LRIM1 and APL1. Knockdown of either of the two LRR-encoding genes depletes mature TEP1 from the hemolymph, probably as a result of its misguided binding to self-tissues, and abolishes TEP1 binding to *P. berghei*. Our results demonstrate that the expression and function of three major antiparasitic factors are coordinated in a complement-like cascade that represents a crucial component of *Plasmodium* killing, and that LRR proteins function as complement-control proteins in the mosquito.

RESULTS

Coregulation of *TEP1*, *LRIM1*, and *APL1* Expression by the Cactus/Rel1 Signaling Module

Expression of genes involved in the same functional pathways is often coregulated at the transcriptional level. We have previously reported that basal levels of expression of *TEP1* and *LRIM1*, but not of *APL1*, are regulated by the NF-κB factor Rel1 and its inhibitor, Cactus (Frolet et al., 2006). Given strong functional indications that these three genes might function in the same pathway, we re-examined the *APL1* expression pattern based on the analysis of *APL1* clones identified in a cDNA library of mosquito hemocytes and midguts (S. Wyder, S.-H. Shiao, S.A.B., C. Kappler, C.F., N. Baldeck, J.A.H., and E.A.L., unpublished data). Four cDNA clones corresponded to *APL1* as it was formerly annotated by the Ensembl database (ENSANGT00000014508) (Riehle et al., 2006). Sequence analysis showed that this initial prediction for *APL1* comprised at least two distinct genes. Two clones (4CE12 and 63BH09) represent one gene, annotated now as AGAP007037. Expression of this gene was tested previously (Frolet et al., 2006) and was not affected by *dsAPL1* knockdown. Clones 104AF09 and 11CC06 encode the *APL1* gene (AGAP007033) against which dsRNA had been designed (Riehle et al., 2006). We re-examined the expression of *APL1* in *Cactus*- and *Rel1*-deficient backgrounds using the updated sequence information. A 3-fold boost of *APL1* expression was observed 4 days after *dsCactus* injection compared to the control *dslacZ* (Figure 1A). Simultaneous silencing of *Cactus* with *Rel1* rescued

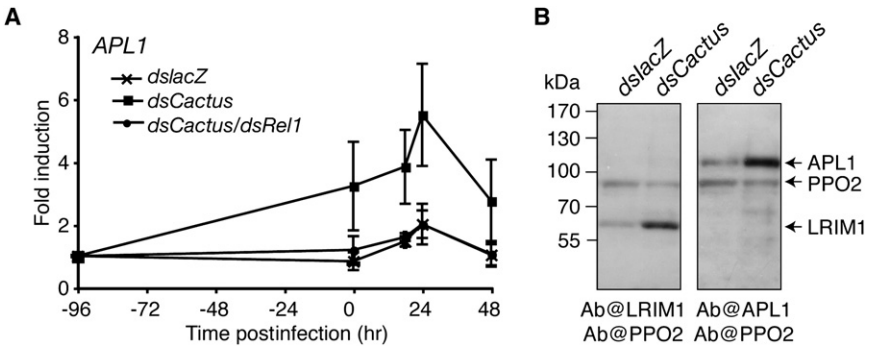

Figure 1. Regulation of *APL1* and *LRIM1* Expression by the Cactus/Rel1 Cassette

(A) Transcriptional profiling of *APL1* in dsRNA-treated mosquitoes by quantitative real-time PCR. Mosquitoes were injected with dsRNA and infected with *P. berghei* 4 days later. Relative transcript levels were assessed before dsRNA injection (−96 hr) and at 0, 18, 24, and 48 hr post-infection (ten mosquitoes per data set). Data was normalized using ribosomal protein transcript *RpL19*, and fold induction was calculated relative to the *APL1* expression levels before dsRNA injection. Mean values ± SEM of two or three independent biological experiments are shown.

(B) Immunoblotting of hemolymph collected from 15 *dslacZ*- and *dsCactus*-treated mosquitoes 4 days after injection using anti-LRIM1 and anti-APL1 antibodies. Antibody against secreted PPO2 was used as a loading control.

the effect of *Cactus* knockdown, demonstrating that the Cactus/Rel1 cassette regulates the levels of expression of *APL1*. Interestingly, after *P. berghei* infection, the pattern of expression of *APL1* was similar to that of *TEP1* and *LRIM1* (Blandin et al., 2004; Frolet et al., 2006), with a peak of expression at 24 hpi.

We raised rabbit polyclonal antibodies against LRIM1 and APL1 to monitor their expression at the protein level. Using these antibodies for immunoblotting analysis, signals corresponding to secreted LRIM1 (~60 kDa) and APL1 (~100 kDa) were detected in hemolymph extracts. Importantly, a prominent increase in the intensity of LRIM1 and APL1 signals, as compared to *dslacZ* controls, was observed in hemolymph extracts from *Cactus* knockdown mosquitoes 4 days after dsRNA injection (Figure 1B). Thus, expression of *TEP1*, *LRIM1*, and *APL1* is coregulated by the Rel1/Cactus signaling module. Our results on *APL1* expression are consistent with a recent independent report (Riehle et al., 2008).

LRIM1 and APL1 Are Required for TEP1 Binding to Ookinetes

We next examined whether the function of TEP1 is preserved in LRIM1- and APL1-depleted backgrounds by monitoring the efficiency of TEP1 binding to ookinetes. To this aim, we silenced *LRIM1* and *APL1* by injection of dsRNA. Injection of *dslacZ* served as a negative control for the effect of injury and dsRNA treatment. Four days after injection, mosquitoes were infected with a *GFP*-expressing *P. berghei* strain by taking a blood meal on an infected mouse (Franke-Fayard et al., 2004). TEP1 binding to ookinetes was monitored 18 and 24 hpi by immunostaining of midguts with polyclonal antibody raised against a C-terminal portion of TEP1 (Levashina et al., 2001). As previously reported for *dslacZ*-injected control mosquitoes, approximately 5% and 30%–50% of parasites displayed TEP1 staining on their surface at 18 and 24 hpi, respectively (Frolet et al., 2006). Most TEP1-positive parasites no longer expressed *GFP* and were considered dead (Figure 2A). Remarkably, *LRIM1* and *APL1* single and *LRIM1*/*APL1* double knockdowns completely abolished TEP1 binding to parasites, demonstrating that LRR proteins are required for TEP1 function.

The striking absence of TEP1 on the parasite surface in the LRIM1- and/or APL1-depleted mosquitoes could result from reduced *TEP1* expression. To test this, the presence of TEP1 protein in hemocytes was examined at 18 hpi. A signal corresponding to TEP1 was detected in all tested knockdowns (Figure 2B), suggesting that *dsLRIM1* and/or *dsAPL1* do not affect *TEP1* expression at the protein level. These results were independently confirmed at the transcriptional level by quantitative real-time PCR (Figure 2C). Depletion of LRIM1 or APL1 did not decrease levels of *TEP1* expression at 48 hr after dsRNA injection, and a consistent albeit modest increase in *TEP1* expression was detected in *dsLRIM1*/*dsAPL1* double knockdown mosquitoes. We conclude that LRIM1 and APL1 do not regulate *TEP1* expression, but its posttranslational activity.

LRIM1 and APL1 Stabilize the Circulating Cleaved TEP1

Proteolytic activation plays a crucial role in the function of complement proteins (Lachmann and Hughes-Jones, 1984). To examine whether LRIM1 and APL1 affect TEP1 cleavage after *Plasmodium* infection, protein extracts of mosquito hemolymph were analyzed by immunoblotting with our existing C-terminal polyclonal antibodies (Levashina et al., 2001) and a specific monoclonal antibody raised against a peptide from the N-terminal portion of TEP1s. In these experiments, we included an additional negative control by injecting dsRNA targeting another LRR-encoding gene, *APL2*, whose silencing has no effect on parasite development (Riehle et al., 2006). In all tested knockdowns, the signal corresponding to the full-length form of TEP1 (TEP1-F) was not significantly affected (Figure 3A). In contrast, silencing of *LRIM1* and *APL1*, but not of *APL2*, severely reduced the signal corresponding to TEP1-C in hemolymph extracts. Similar results were obtained for TEP1-N, indicating that depletion of LRR proteins interferes either with TEP1 cleavage or with the stability of its processed forms. We also noted that the phenotype of concomitant silencing of *LRIM1* and *APL1* was comparable to single knockdowns (data not shown). The effect of LRIM1 or APL1 depletion on the cleaved forms of TEP1 was infection independent, as signals for both cleavage products were reduced before and after *Plasmodium* infection. Strikingly, when protein extracts of whole bodies were examined, all forms (full-length, TEP1-N, and TEP1-C) were detected in control and LRR-depleted mosquitoes (Figure 3B). In these samples, antibodies against TEP1-C were more efficient in recognizing TEP1-C than the full-length form,

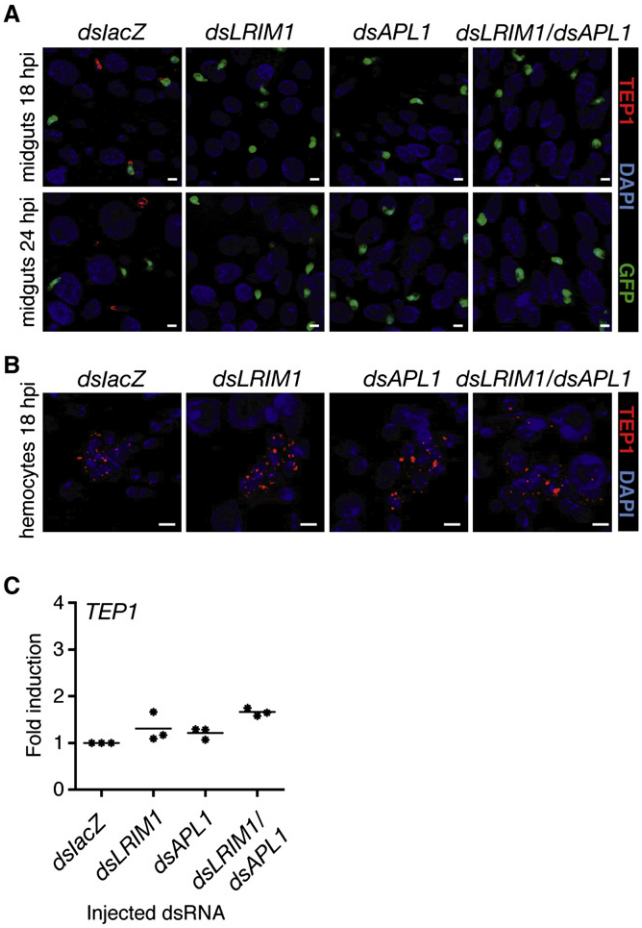

Figure 2. Effect of *LRIM1* and *APL1* Silencing on TEP1 Binding to *P. berghei* and on *TEP1* Levels of Expression

(A and B) Immunofluorescence analysis of midguts (A) and abdominal epidermis with attached hemocytes (B) performed with TEP1-C-specific antibody (red). Mosquitoes were injected with dsRNA, infected with *P. berghei*-GFP (green) 3 days later, and dissected 18 and 24 hr postinfection. Nuclei are stained with DAPI (blue). Images are projections of six to twelve 1.2 μm spaced optical sections. Basal membrane was excluded from the sections. Scale bar: 5 μm.

(C) Transcriptional levels of *TEP1* in dsRNA-treated mosquitoes assessed by quantitative real-time PCR 48 hr after dsRNA injection (ten mosquitoes per data set). Each star represents the levels of *TEP1* transcripts normalized using ribosomal protein gene *RpL19* and expressed as a fold induction relative to the levels of *TEP1* in the *dsLacZ*-injected control. Results of three independent biological experiments are presented.

whereas anti-TEP1-N antibodies readily detected the full-length form and were less efficient in recognizing TEP1-N. Altogether, these results suggest that cleavage of TEP1 is independent of LRIM1 and APL1 function. Instead, the LRR proteins appear to maintain the cleaved form of TEP1 in circulation, as in their absence both TEP1-N and TEP1-C forms, but not the full-length form, are depleted from the hemolymph.

We next sought to identify the site of deposition of TEP1 cleavage products detected in whole-body mosquito extracts. To this end, we performed immunofluorescence analysis of mosquito whole-body preparations using the anti-TEP1-C and anti-TEP1-N antibodies, which allowed us to follow the fate of each of the two moieties of the cleaved TEP1. Unlike control mosquitoes displaying low background fluorescence, colocalization of TEP1-N- and TEP1-C-specific signals was detected on the midgut and on the abdominal epidermis of LRIM1- and APL1-depleted mosquitoes (Figures 3C and 3D). As *LRIM1* and *APL1* knockdowns did not affect the presence of full-length TEP1 in circulation (Figure 3A), we interpret the colocalization of the two signals as the deposition of the cleaved form of TEP1 on mosquito tissues. TEP1 was observed on self-tissues for at least 8 days with no adverse effects on mosquito survival (data not shown).

We extended this analysis to TEP1 binding to parasites. Coimmunostaining experiments with the anti-TEP1-N and anti-TEP1-C antibodies revealed a perfect colocalization of TEP1-N and TEP1-C signals on the surface of dead and dying parasites at 24 hpi (Figure 3E). Taken together, our results demonstrate that the full-length form of TEP1, TEP1-F, does not bind to parasites in LRR-depleted mosquitoes. Thus, either LRR proteins are required for TEP1-F binding to parasites, or it is the cleaved form of TEP1 that decorates invading parasites.

Proteolytic Cleavage of Recombinant TEP1 In Vitro Produces a Two-Chain Molecule

Our observations of colocalization of the immunofluorescence signals for N- and C-terminal fragments of TEP1 on ookinetes and self-tissues, together with our previous structural analysis (Baxter et al., 2007), suggest that proteolytic cleavage of circulating TEP1 in vivo does not lead to dissociation of the two fragments, but rather converts the full-length form into a two-chain molecule. To test this prediction, we characterized TEP1 after proteolytic cleavage in vitro using protein from the refractory L3-5 mosquito strain that was recombinantly produced incorporating a C-terminal histidine-tag (TEP1r-6×His) and purified to homogeneity as previously described (Baxter et al., 2007). We have previously shown by protein sequencing that trypsin processes TEP1 after residue 601 (Baxter et al., 2007), producing the same-sized N-terminal (75 kDa) and C-terminal (85 kDa) fragments as observed for TEP1 in vivo (Levashina et al., 2001). Therefore, we performed limited trypsinolysis on purified recombinant TEP1r-6×His and compared the full-length and cleaved forms by chromatography. The N- and C-terminal fragments comigrated in size-exclusion chromatography with the same apparent molecular weight as full-length TEP1r-6×His (Figure 4A), and both fragments eluted at the same ionic strength in cation-exchange chromatography (Figure 4B). These results indicate that both chains of TEP1 remain associated after cleavage in vitro.

The protease responsible for TEP1 cleavage in vivo has not yet been identified and may have different substrate specificity to trypsin, which cleaves after basic residues. Structural analysis predicted that the TEP1 protease-sensitive region spans residues 580–601 and contains multiple cleavage sites for a variety of proteases. Therefore, we performed limited proteolysis of TEP1r-6×His with chymotrypsin (cleaving after aromatic residues), elastase (cleaving after small hydrophobic residues), and *S. aureus* V8 protease (cleaving after acidic residues) and analyzed the results by SDS-PAGE. TEP1r-6×His was readily cleaved by trypsin, chymotrypsin, and elastase (Figure 4C, data not shown for elastase), generating N- and C-terminal

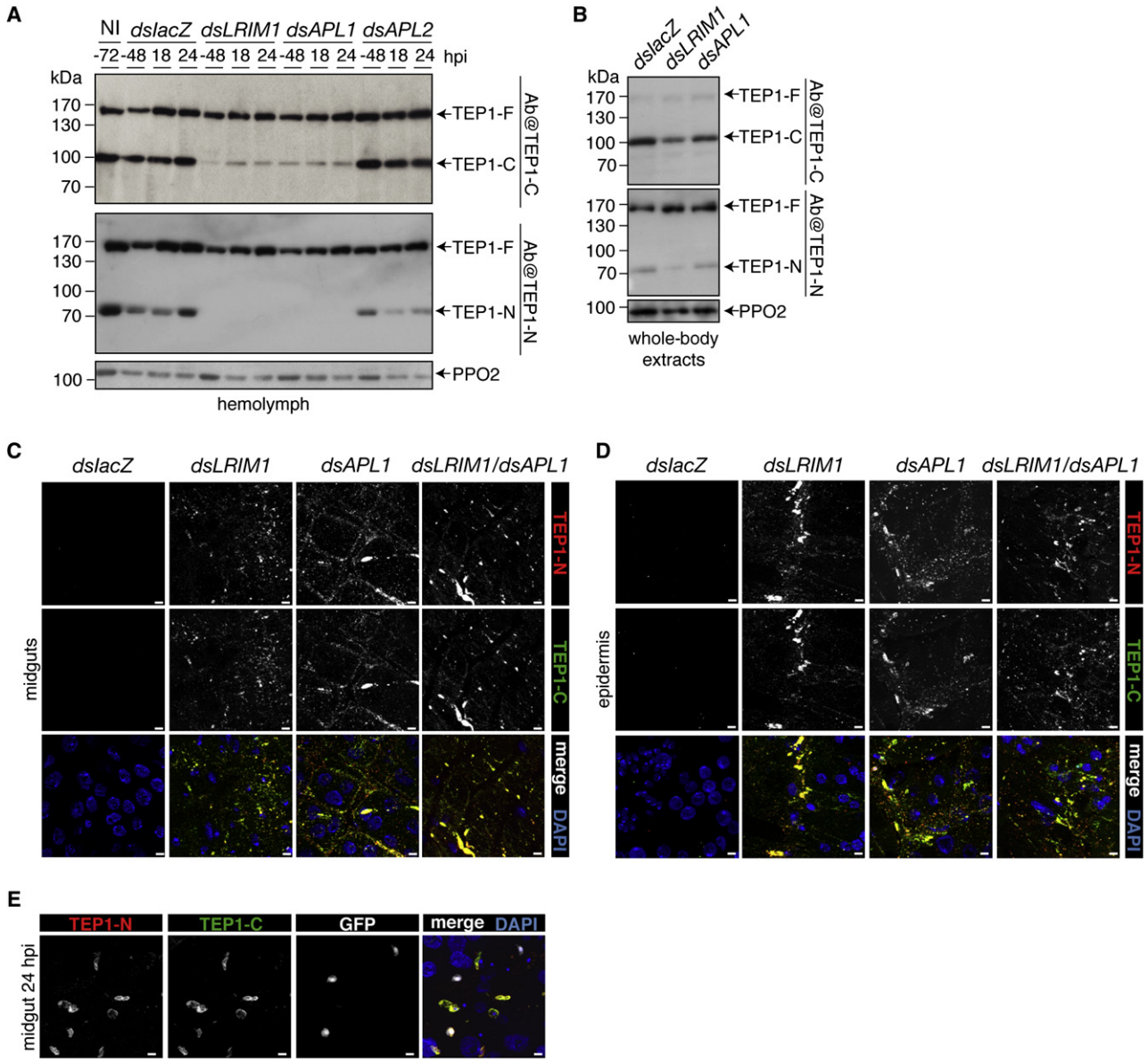

Figure 3. Effect of LRIM1 and APL1 Depletion on TEP1 Maturation and Binding Properties

(A) Immunoblotting of hemolymph collected from noninjected (NI) and dsRNA-treated mosquitoes 24 hr after injection and 18 and 24 hr postinfection with *P. berghei* (15 mosquitoes per group). The full form (TEP1-F) and the C-terminal cleaved form (TEP1-C) of TEP1 are revealed on the blots by TEP1-C-specific antibodies. TEP1-F and the N-terminal cleaved form (TEP1-N) of the protein are revealed by TEP1-N specific antibodies.

(B) Immunoblotting of whole-body protein extracts using TEP1-C- and TEP1-N-specific antibodies. Whole-body extracts were prepared by homogenization of tissue from ten mosquitoes collected 24 hr after dsRNA injection. In (A) and (B), antibody against secreted PPO2 was used as a loading control.

(C and D) Immunostaining of midguts (C) and abdominal epidermis (D). TEP1 signal corresponding to the TEP1-N-specific antibody is shown in red and staining with the TEP1-C-specific antibody in green. Mosquitoes were dissected 24 hr after dsRNA injection. Nuclei are stained with DAPI (blue). Images are projections of four to six 1.2 μm spaced optical sections. Note that in contrast to the images shown in Figures 2A and 3E, basal membrane is included in the reconstruction of optical sections. Scale bar: 5 μm.

(E) Colocalization of TEP1-N and TEP1-C on ookinetes. Immunostaining of infected midguts with TEP1-N (red)- and TEP1-C (green)-specific antibodies. Mosquitoes were infected with *P. berghei*-GFP (white), and midguts were dissected 24 hpi. Nuclei are stained with DAPI (blue). Images are projections of twelve 1.2 μm spaced optical sections. Scale bar: 5 μm.

fragments that were stable in an excess of these two proteases and sized similarly to those seen in vivo. In contrast, V8 protease did not cleave TEP1r-6×His at low concentrations and, in excess, led to fragments distinct from those observed in vivo, despite the presence of an acidic residue (Glu585) within the predicted range of residues 580–601. Thus we predict that, like trypsin, the endogenous protease(s) for TEP1 cleave(s) within residues 585–601 of the protease-sensitive region and that, in

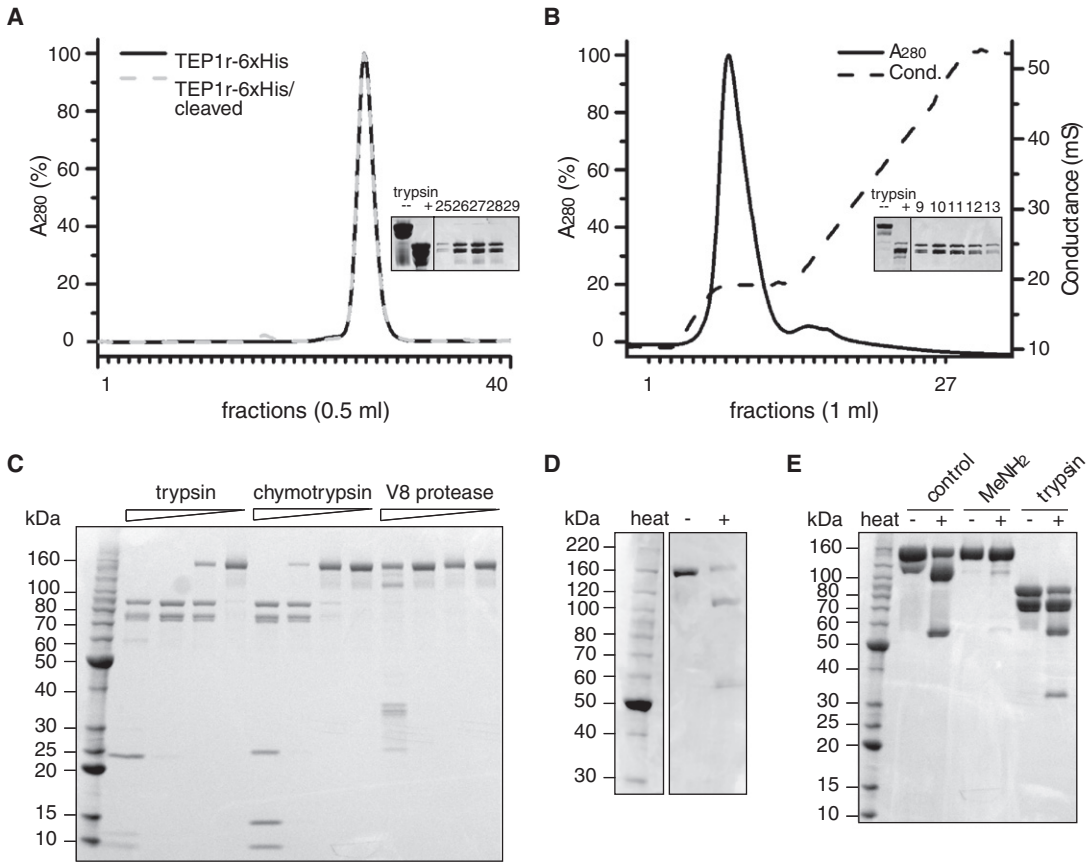

Figure 4. Proteolytic Cleavage of Recombinant TEP1 In Vitro and Biochemical Properties of the Resulting Two-Chain Molecule

(A) Purification of full-length and trypsinized (cleaved) TEP1r-6×His by size-exclusion chromatography. Inset shows Coomassie-stained SDS-PAGE of the loaded protein for TEP1r-6×His, cleaved TEP1r-6×His, and five peak fractions (0.5 ml each) for cleaved TEP1r-6×His.

(B) Purification of trypsinized TEP1r-6×His by cation-exchange chromatography. The solid line plot represents relative absorbance (left axis) and the dashed line conductivity (right axis). Inset shows Coomassie-stained SDS-PAGE of protein before and after limited trypsinolysis and five peak fractions (1 ml each).

(C) Limited proteolysis of purified TEP1r-6×His. Coomassie-stained SDS-PAGE of TEP1r-6×His treated with trypsin, chymotrypsin, and *S. aureus* V8 protease; gradient shows decrease in protease concentrations from 1:1000 to 1:1 weight protein:protease ratio.

(D) Thioester assay for soluble TEP1r-6×His, stored at room temperature for 54 days.

(E) Thioester assay for purified TEP1r-6×His. Coomassie-stained SDS-PAGE of control (–) and heat-exposed test (+) samples for TEP1r-6×His, treated with methylamine ($MeNH_2$) at pH 9.5 and following limited trypsinolysis. Methylamine treatment inactivates the thioester, thereby preventing the autolytic cleavage of full-length TEP1r-6×His. An active thioester is retained in trypsinized TEP1r-6×His, evidenced by autolysis of the 85 kDa C-terminal fragment into 55 kDa (residues 841–1325) and 30 kDa (residues 601–840) fragments. Molecular weight markers for (C)–(E) are BenchMark unstained protein ladder (Invitrogen).

this respect, trypsinized TEP1 mimics the in vivo cleaved form. The general proteolytic susceptibility within this region is more similar to α_2-macroglobulin than to complement factors.

Proteolysis of TEP1 may lead to (1) maturation (for instance, intracellular processing of complement factors), which leaves the thioester bond intact, or (2) activation (for instance, cleavage of the bait region of α_2-macroglobulin), causing dramatic structural changes and rapid reaction of the thioester. Proteolysis of complement factor C3 by either its native convertase or by trypsin leads to rapid (<1 s) activation to C3b (Sim et al., 1981). To determine if cleavage of TEP1r-6×His in the protease-sensitive region results in its activation, we assayed the presence of an intact thioester bond in the full-length and cleaved forms by heat-induced autolytic cleavage of denatured protein (Sim and Sim, 1981). We had shown that, upon heating, the intact protein (160 kDa) was cleaved at Gln841 of the full-length protein, generating an N-terminal (105 kDa) and a C-terminal (55 kDa) fragment (Levashina et al., 2001). As a control, we inactivated the thioester bond with methylamine at alkaline pH. Purified full-length TEP1r-6×His readily underwent autolytic cleavage after heat treatment, demonstrating that it contained an intact thioester bond (Figure 4D). Methylamine treatment efficiently inactivated the thioester bond in purified TEP1r-6×His, as evidenced by absence of autolytic cleavage. Binding of methylamine to Gln841 was confirmed by mass spectrometry (data not shown). Upon limited proteolysis with trypsin, however, fragmentation of the C-terminal 85 kDa band was still observed upon heating, indicating the presence of an intact thioester. Hence, cleavage of TEP1r-6×His within the protease-sensitive region is not sufficient to cause spontaneous activation of the thioester bond. Together, our in vitro results support a model whereby proteolytic cleavage of TEP1 in vivo generates a mature two-chain molecule that retains the capacity for covalent attachment to a substrate.

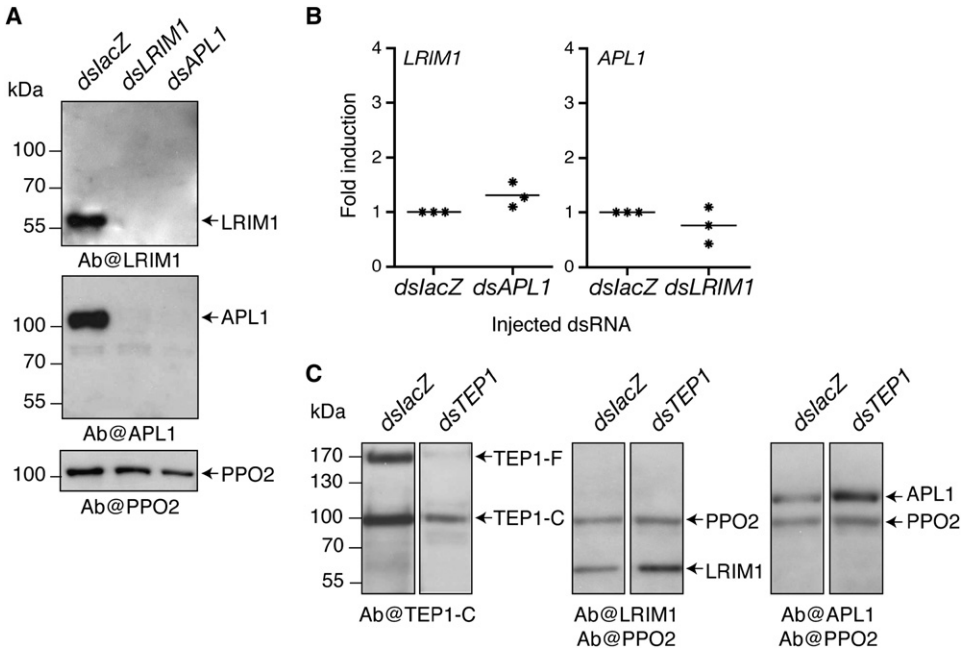

Figure 5. Expression and Protein Profiles of LRIM1 and APL1 in Different Knockdown Backgrounds

(A) Immunoblotting of hemolymph samples collected from 15 dsRNA-injected mosquitoes 24 hr postinjection. The hemolymph profiles of LRIM1 and APL1 are presented. Antibody against secreted PPO2 was used as a loading control.

(B) Transcriptional profiling of *LRIM1* and *APL1* in dsRNA-treated mosquitoes by quantitative real-time PCR 48 hr after dsRNA injection (ten mosquitoes per data set). Each star represents transcript levels of the analyzed gene normalized to the levels of the ribosomal protein transcript *RpL19* and expressed as fold induction relative to the levels of each gene in the *dslacZ*-injected control. Results of three independent biological experiments are plotted.

(C) Immunoblotting of hemolymph extracts collected from 15 mosquitoes 4 days after dsRNA injection. The hemolymph profiles of TEP1, LRIM1, and APL1 are shown. Note that the same membranes were used to probe the antibodies. Antibody against secreted PPO2 was used as a loading control.

LRIM1 and APL1 Stabilize Each Other Prior to Interaction with TEP1

Expression of both *LRIM1* and *APL1* is required to prevent deposition of mature TEP1 on self-tissues after proteolytic cleavage, pointing out that the functions of these two genes might be tightly linked. We monitored by immunoblotting the presence of LRIM1 and APL1 in the hemolymph extracts of a series of knockdown backgrounds using the polyclonal antibodies raised against both proteins (Figure 5A). Knockdown of *LRIM1* and *APL1* efficiently depleted the corresponding signals, indicating that gene silencing was successful. Unexpectedly, knockdown of *APL1* caused complete disappearance of the signal corresponding to LRIM1 and, reciprocally, knockdown of *LRIM1* eliminated APL1. To eliminate the possibility of RNAi-induced cross-silencing, we gauged levels of *LRIM1* and *APL1* expression after dsRNA injection by quantitative real-time PCR. No significant differences were observed in the *LRIM1* transcript levels in *APL1*-deficient mosquitoes compared to the control *dslacZ*. Similarly, the transcription of *APL1* in *dsLRIM1*-injected mosquitoes was not notably altered (Figure 5B), ruling out the possibility of RNAi cross-silencing. Our findings suggest that the two LRR proteins are unstable individually and require the presence of each other to persist in circulation, perhaps through the formation of a complex. These results are in line with striking similarities between single and double knockdown phenotypes of the LRR-encoding genes. Indeed, a single knockdown of either *LRIM1* or *APL1* is sufficient to entirely remove both proteins from circulation and therefore is phenotypically equivalent to a double knockdown.

We next examined whether persistence of LRR proteins in the hemolymph depends on TEP1. Both LRIM1 and APL1 were detected in the hemolymph of *TEP1*-knockdown mosquitoes; therefore, the stability of LRRs does not require TEP1 presence (Figure 5C).

LRIM1 and APL1 Interact with TEP1

To determine whether the two LRR proteins may interact with TEP1, we carried out coimmunoprecipitation (co-IP) experiments. In mosquitoes, co-IP of hemolymph proteins is often hampered by limited quantities of available biological material. To bypass this constraint, we directly injected adult females with purified full-length TEP1r-6×His (Figure 6A). PBS-injected mosquitoes served as a negative control, as all our attempts to use unrelated 6 × His-tagged proteins were unsuccessful (failure to immunoprecipitate the exogenous protein). TEP1-interacting proteins are expected to bind the injected TEP1r-6×His fusion protein and to be pulled down with it. Protein extracts of injected mosquitoes were prepared 3 hr after injection, and IP was performed with anti-6×His-tag antibody. Immunoprecipitates and post-IP samples were analyzed by immunoblotting using antibodies against the 6×His-tag, TEP1-C, TEP1-N, LRIM1, APL1, and pro-phenoloxidase 2 (PPO2) (Figure 6B). TEP1r-6×His was rapidly processed in the mosquito body cavity, and its C-terminal cleaved form was detected in the precipitates

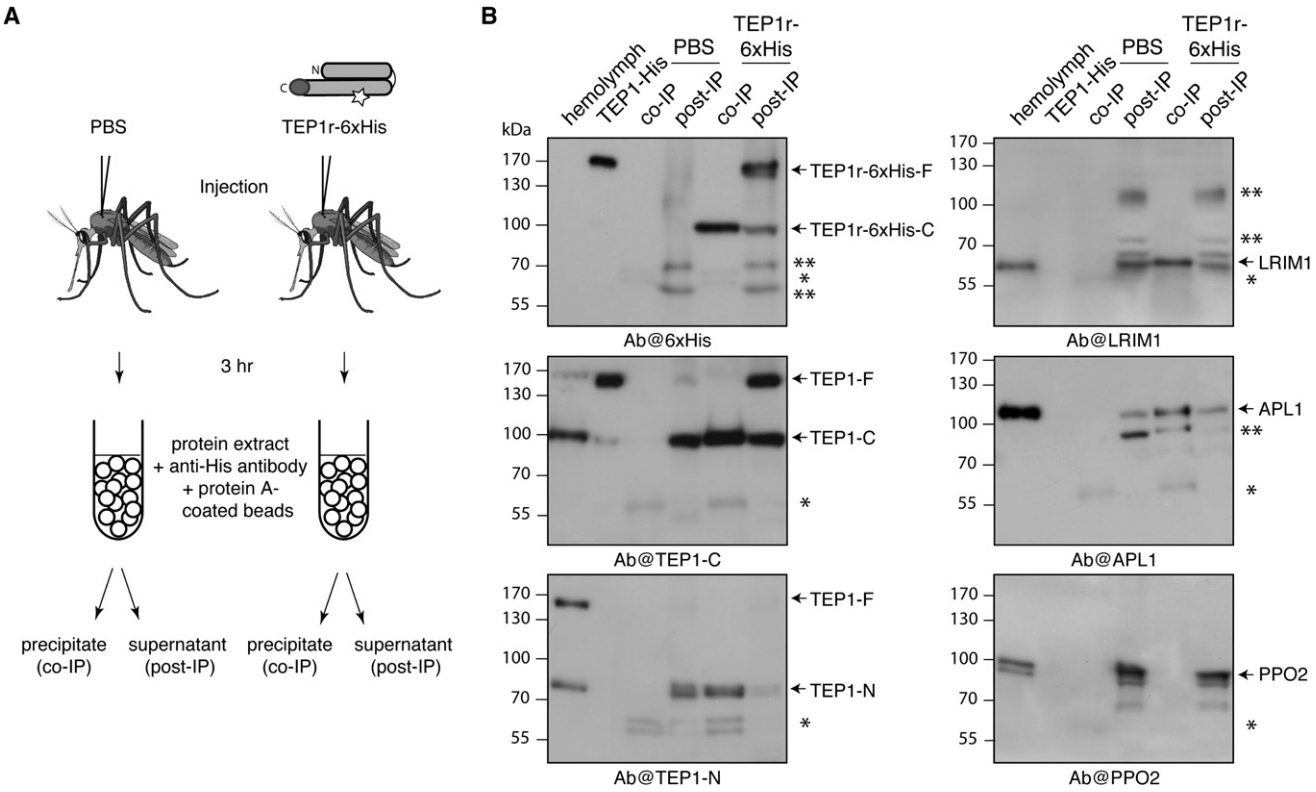

Figure 6. Coimmunoprecipitation Analysis of TEP1, LRIM1, and APL1 Interactions

(A) Experimental setup. Mosquitoes were injected with either recombinant TEP1r-6×His dissolved in PBS or with PBS only and collected 3 hr later for tissue homogenization and lysis. Injected TEP1r-6×His was immunoprecipitated with anti-6×His-tag antibody.

(B) Immunoblotting analysis of postimmunoprecipitation lysate (post-IP) and precipitates (co-IP). Hemolymph and TEP1r-6×His protein served as a positive control. The membrane was probed with antibodies specific for the 6×His-tag, TEP1-C, TEP1-N, LRIM1, APL1, and PPO2. *, heavy chains of the mouse anti-6×His-tag antibody recognized by secondary anti-mouse IgG antibody or crossreacting anti-rabbit IgG antibody; **, nonspecific signals observed in post-IP and co-IP samples.

from TEP1r-6×His-injected but not PBS-treated mosquitoes. The full form of the fusion protein was not retained by the antibody and remained in the post-IP supernatant. Importantly, a signal corresponding to LRIM1 and APL1 was revealed in the precipitates from TEP1r-6×His-injected mosquitoes but was absent in control samples, demonstrating that the two LRR proteins coimmunoprecipitated with TEP1-C in our experimental settings. We next investigated whether endogenous TEP1 was also precipitated. To distinguish between the recombinant and endogenous TEP1, we made use of the TEP1-N monoclonal antibody, which specifically recognizes endogenous TEP1s from the G3 mosquitoes but not TEP1r from the L3-5 strain or recombinant TEP1r-6×His (Figures 6B and S1). Endogenous TEP1-N was detected in the immunoprecipitate, suggesting that in addition to LRIM1 and APL1, the protein complex contains more than one TEP1 molecule. As a control for the specificity of IP, we reprobed the immunoblots with an antibody against PPO2, a hemolymph-borne enzyme catalyzing melanization reaction in insects, which we have used as a loading control throughout this study. Although a clear PPO2-positive signal was detected in the post-IP samples, it was not observed in the IP precipitates, indicating that TEP1r-6×His pull-down was specific. We conclude that the stabilization of mature TEP1 in the hemolymph requires a multiprotein interaction involving several TEP1 molecules and at least two LRR proteins, LRIM1 and APL1.

DISCUSSION

The ability to detect and swiftly destroy invading pathogens is of paramount importance to any living organism. Several factors have been identified in mosquitoes that are required for efficient *Plasmodium* elimination. However, how the functions of these factors converge to ensure parasite killing has remained unclear. Here, we report that binding of TEP1 to the parasite surface, a crucial event in *Plasmodium* killing, requires the coordinated action of LRIM1 and APL1. Silencing of either of the two LRR-encoding genes leads to deposition of cleaved TEP1 on self-tissues, resulting in depletion of the protein from circulation and to the abolishment of TEP1 binding to ookinetes and their subsequent lysis during *Plasmodium* infection. Therefore, the high oocyst survival reported in LRIM1- and APL1-depleted mosquitoes (Osta et al., 2004; Riehle et al., 2006) can be predominantly if not completely attributed to the malfunction of TEP1.

TEP1 shares significant sequence similarity and structural organization with the mammalian complement factor C3 (Baxter et al., 2007; Levashina et al., 2001). In mammals, intracellular

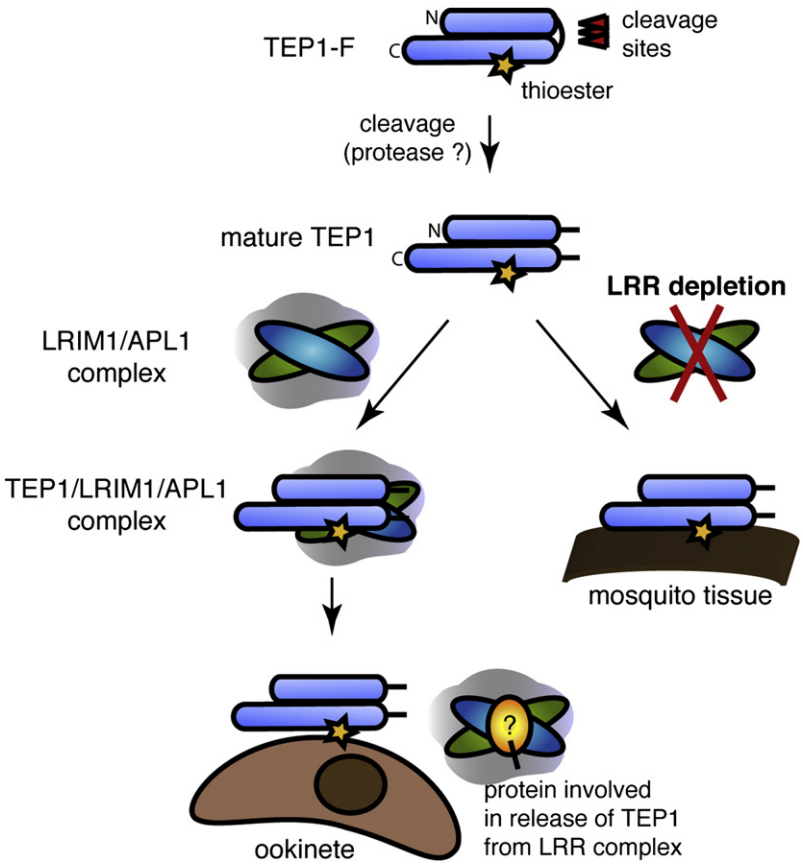

Figure 7. Model for TEP1 Function in the Presence and Absence of the LRIM1/APL1 Complex

TEP1, which has several potential cleavage sites, is constitutively cleaved in the hemolymph by (an) as yet unknown protease(s). The processing generates TEP1-N and TEP1-C fragments, which remain associated as two chains. The mature form of TEP1 is maintained in circulation by a complex composed of the LRR proteins LRIM1 and APL1 (the complex stoichiometry is not considered). During infection with *P. berghei*, the LRR complex is displaced from TEP1, which binds to the parasites and promotes their killing. When LRR-encoding genes are silenced by RNAi, mature TEP1 is depleted from circulation by deposition on self-tissues before it could bind parasites.

maturation of C3 produces a two-chain molecule, which is secreted into the blood. Further proteolytic cleavage releases the N-terminal fragment of the α chain, C3a, thus bringing about major structural changes and causing the binding of C3b to nearby pathogen surfaces. The soluble C3a anaphylatoxin signals to immune cells to attract them to the site of C3 activation. In contrast to C3, TEP1 is secreted into hemolymph as a single chain molecule. The cleavage of TEP1 in the protease-sensitive region is functionally reminiscent of the intracellular maturation of C3: in both cases, the cleaved products remain associated to form a two-chain molecule, which retains the intact internal thioester bond. In the case of TEP1, however, this maturation takes place in the hemolymph and not intracellularly. The cleavage is brought about by as yet unknown secreted protease(s), which cleave(s) TEP1 within the 20-amino-acid protease-sensitive region. Therefore, the crystal structure of TEP1r may indeed represent a proform as has been suggested (Gros et al., 2008). It is presently unclear how activation of mature TEP1 is achieved and whether, similarly to C3, an additional cleavage is required for this process.

The LRR protein-deficient model provides an excellent tool to dissect early stages of TEP1 activation. The correlation between abolition of TEP1 binding to parasites and depletion of the mature form of TEP1 from circulation suggests that full-length TEP1, present in the hemolymph, requires maturation to adopt binding capability. New tools are necessary, however, to firmly establish in vivo that it is indeed the mature two-chain and not the full-length form that binds to parasites and self-tissues.

TEP1 is maintained in circulation by interaction with LRIM1 and APL1. If either of the LRR proteins is removed, the cleaved form of TEP1 disappears from circulation, and massive deposition of TEP1 on self-tissues is detected, suggesting that LRR proteins prevent binding of the mature molecule to nearby surfaces. The observation that, in the absence of LRRs, TEP1 binds to self-surfaces before *Plasmodium* infection suggests the mosquito origin of TEP1 activators. A number of mammalian complement control proteins that shape binding specificities of complement factors have been identified (Liszewski et al., 1996), and here we implicate LRR proteins in this process. The role of LRR proteins revealed by this study might be also relevant for regulation of complement factors in other organisms.

Results presented here lead us to propose the following model of TEP1 activation (Figure 7). TEP1 is constantly cleaved in the hemolymph by (an) as yet unknown endogenous protease(s), producing a mature cleaved molecule. Our structural and biochemical studies in vitro strongly suggest that the N- and C-terminal fragments do not dissociate after cleavage due to: (1) the MG6 domain, which comprises β strands from both N and C chains, and (2) the tight packing of MG7/MG8 to the other MG domains (Baxter et al., 2007).

Mature TEP1 readily binds nearby surfaces and becomes depleted from circulation unless it is stabilized by interaction with at least two LRR proteins. LRIM1 and APL1 circulate in the hemolymph and bind TEP1 before or shortly after its proteolytic cleavage. It is currently unclear how the LRR proteins interact. This could be achieved via heterodimerization of LRR domains, as is the case of Toll and Toll-like receptors. Alternatively, their predicted C-terminal coiled-coil motifs may associate with each other to form homo- or heterodimers. Still, whether the two LRR proteins form a complex and its molecular composition remain to be elucidated. How TEP1 is targeted to the parasite surface also requires clarification. A possible mechanism could be through displacement of the LRR proteins from TEP1 as a result of direct or indirect interaction of LRR proteins with (a) parasite protein(s) or by their proteolytic degradation. Thus, LRR proteins might play a dual role in the process: (1) as

complement control proteins that prevent inappropriate activation of TEP1 and (2) as recognition or guard molecules that control TEP1 binding to pathogens. Our model further supports the recently established concept of basal immunity in *A. gambiae* (Frolet et al., 2006). Indeed, the function of LRIM1 and APL1 is required prior to infection to maintain an appropriate level of mature TEP1 in circulation.

Taken together, these data integrate previously identified players into one major pathway employed by mosquitoes to reduce the burden of *Plasmodium* infection and provide insights into the regulation of TEP1 attachment to the parasites. All refractory phenotypes described to date exhibit faster TEP1 binding and complete *Plasmodium* killing at the very early time points of infection (Blandin et al., 2004; Frolet et al., 2006). Further dissection of molecular mechanisms that govern efficiency of TEP1 deposition on the parasite surface will be an asset for design of novel strategies for vector control based on modulation of the mosquito immune defense. Importantly, this defense appears to be relevant not only for the rodent malaria model used in this study, but also for human malaria parasites.

EXPERIMENTAL PROCEDURES

Mosquito Rearing and Parasite Infections

A. gambiae G3 (S) and L3-5 (R) strains were maintained at 28°C and 70%–80% humidity in a 12/12 hr day/night cycle. For infection experiments, mosquitoes were fed on anesthetized CD1 mice infected with the *P. berghei* GFP-con 259cl2 clone (ANKA strain) that constitutively expresses *GFP* (Franke-Fayard et al., 2004). Unfed mosquitoes were removed from the samples. Parasitemia in mice was assessed by Diff-Quick I- and II- (eosin G and thiazine dye, Dade Behring) stained smears from tail blood for proportion of infected red blood cells and gametocytes and/or by FACS analysis of GFP parasites.

DsRNA Synthesis and Injection

A fragment of *APL1* and of *APL2* was amplified by PCR from cDNA templates of G3 mosquitoes using specific primer pairs and conditions reported earlier (Riehle et al., 2006). The *APL1* PCR product was cloned into the pGEM-T Easy Vector and subcloned into pLL10 (Blandin et al., 2002) as a 613 bp EcoRI fragment, resulting in pLL442. The *APL2* PCR product was cloned into the pGEM-T Easy Vector and subsequently cloned into pLL10 as an 882 bp EcoRI insert, producing pLL444. Production of dsRNA was carried out as previously reported (Frolet et al., 2006; Levashina et al., 2001).

For RNAi gene silencing, 1- to 2-day-old females were anesthetized on a CO_2 pad and injected with 138 nl of *dslacZ* or a mixture of two different dsRNAs at a concentration of 3 μg/μl using a Nanoject II Injector (Drummond; Broomall, PA). In order to inject the same quantity and volume of dsRNA while performing single and double gene knockdowns, dsRNAs for single knockdowns were mixed with *dslacZ* in a 1:1 proportion. For *P. berghei* infection experiments, mosquitoes recovered for 3 days following injection before being offered an infectious blood meal.

Phenotypic Analysis after dsRNA Injection

Immunoblotting

Hemolymph was collected in denaturing protein loading buffer (Tris-HCl 0.35 M, SDS 10.3%, glycerol 36%, β-mercaptoethanol 5%, bromophenol blue 0.012%) by proboscis clipping from 10 or 15 dsRNA-treated mosquitoes at different time points after injection and/or infection. For whole-body mosquito extracts, ten insects were ground in extraction buffer containing 20 mM HEPES pH 7.5, 1 M NaCl, and a protease inhibitor cocktail (Complete Mini, Roche). Debris and lipids were removed by centrifugation. Hemolymph and whole-body extracts were denatured in protein loading buffer at 65°C for 5 min. Samples were separated by 7% SDS-PAGE. Protein membrane transfer, antibody incubations, and detection were carried out as previously described (Levashina et al., 2001).

Immunofluorescence Analysis

Mosquito midguts and abdominal epidermis were dissected on ice, fixed in 4% formaldehyde, washed with PBS, and incubated with affinity-purified rabbit polyclonal anti-TEP1-C antibody (1/300) (Levashina et al., 2001) and/or mouse monoclonal anti-TEP1-N antibody (1/20). Secondary fluorescence-labeled antibodies (Cy3 or Alexa546, Alexa488, Cy5) were used at a dilution of 1/1000 (Jackson Laboratory; Bar Harbor, ME). Tissues were mounted in DAPI-containing Vectashield medium (Vector Laboratories, Inc.; Burlingame, CA) and monitored using an Axiovert 200M fluorescence microscope (Zeiss) equipped with an Apotome module (Zeiss). Images of 6–12 optical sections were created, and captures were reconstructed and analyzed using the AxioVision 4.6 software (Zeiss).

Quantitative Real-Time PCR

Total RNA from ten mosquitoes was extracted with TRIzol reagent (Invitrogen) and treated with DNase I (Ambion; Austin, TX) according to the suppliers' instructions. Total RNA (2 μg) was converted to cDNA using the M-MLV Reverse Transcriptase (Invitrogen) and random hexamers (Invitrogen). Quantitative PCR reactions were run on a 7500 Fast Real-Time PCR instrument (Applied Biosystems) using the TaqMan Fast Universal PCR Master Mix (Applied Biosystems) according to the manufacturer's instructions. For *LRIM1* (AGAP006348) and *APL1* (AGAP007033), the PCR reactions were assembled using the ABsolute QPCR SYBR Low ROX mix (Thermo Scientific). Primers and probes were designed with the Primer Express software (Applied Biosystems). The ribosomal protein transcript *RpL19* (AGAP004422) was used as an internal control in all the experiments. Data was analyzed with the Fast Real-Time PCR software (Applied Biosystems).

TEP1: AG486 forward primer 5′-ATACGGATCTCAGCTATACCAAATCG-3′
AG487 reverse primer 5′-TGCGGGCCTTTATGAGAAAA-3′
TaqMan probe 5′-*FAM*-TCCGAAGGTTGGTGTTC-*MGB*-3′
RpL19: AG490 forward primer 5′-CCAACTCGCGACAAAACATTC-3′
AG491 reverse primer 5′-ACCGGCTTCTTGATGATCAGA-3′
TaqMan probe 5′-*VIC*-CAAACTGATCAAGGATG-*MGB*-3′
LRIM1: AG866 forward primer 5′-AACGGACAGCAGCCTAAAGC-3′
AG867 reverse primer 5′-AGATCAAGCTCCTTTACGTTCCA-3′
APL1: AG868 forward primer 5′-CGACAGCCCGAATACAAATGC-3′
AG869 reverse primer 5′-GCACATCGTAGAACACACAGTCGTA-3′

Antibody Production and Purification

Monoclonal Mouse Anti-TEP1-N Antibodies

Monoclonal antibodies were raised against a 6.8 kDa fragment corresponding to the residues 337–398 of the full-length secreted protein: TPAKGITGK VEVSDVGFETTTTSDNDGLIKLELQPSEGTEQLGINFNAVDGFFFYEDVNKVET. This fragment bears four substitutions that differ between TEP1 from the G3 and L3-5 mosquito strains. The corresponding 206 bp fragment was amplified from pLL3 (Levashina et al., 2001) using forward primer 5′-CCATGGGAA CACCGGCTAAAGGCATTAC-3′, reverse primer 5′-GGTACCTTACGTTTCTAC CTTATTCACATCTTCATA-3′, and standard PCR conditions. The amplified product was first cloned into pCR2.1 TOPO (Invitrogen) and then subcloned as a 204 bp NcoI-KpnI fragment into pETM11 derived from pET24d (Novagen). The His-tagged peptide was produced in *E. coli* BL21 (DH3) with chaperones using the two-step system (de Marco, 2007) and purified by immobilized metal-affinity chromatography. Hybridoma cells producing antibodies against the peptide were produced by the European Molecular Biology Laboratory (Heidelberg, Germany) monoclonal antibody facility and subcloned twice to reach monoclonality. Twenty-times-diluted conditioned medium from clone E1D6 was used for immunoblotting and immunofluorescence analysis.

Polyclonal Rabbit Antibodies Directed Against LRIM1, APL1, and PPO2

For protein expression, the coding sequences of *LRIM1*, *APL1*, and *PPO2* were cloned into expression vectors using the Gateway Cloning technology (Invitrogen). *LRIM1*, *APL1*, and *PPO2* were amplified by PCR from clones of a Gateway cDNA immune library (S. Wyder, S.-H. Shiao, S.A.B., C. Kappler, C.F., N. Baldeck, J.A.H., and E.A.L., unpublished data) (clones 11DF10, 104AF09, and 53BA04, respectively) using the primers listed below. PCR products were cloned by recombination into the entry vector pDONR221 (resulting in pLL462, pLL468, and pLL466, respectively). Inserts were then subcloned by recombination into the expression vector pDEST17 (pLL463, pLL469, and pLL467, respectively).

LRIM1: AG722 forward primer 5′-GGGGACAAGTTTGTACAAAAAAGCAGGCTTCCAGGCGTGCCAAGTCGTC-3′
AG723 reverse primer 5′-GGGGACCACTTTGTACAAGAAAGCTGGGTCCTACAGCTGGCTCGCTAAATTCTG-3′
APL1: AG765 forward primer 5′-GGGGACAAGTTTGTACAAAAAAGCAGGCTTCAATTATTGGTATACGGAAGAGCAG-3′
AG766 reverse primer 5′-GGGGACCACTTTGTACAAGAAAGCTGGGTCCTATGCGCATAGACCTAACGC-3′
PPO2: AG724 forward primer 5′-GGGGACAAGTTTGTACAAAAAAGCAGGCTTCAACAATATCTTGGCCCTGTTGC-3′
AG735 reverse primer 5′- GGGGACCACTTTGTACAAGAAAGCTGGGTCCTACGTGGCCGTCTTCATGTTC

LRIM1 (pLL463), *APL1* (pLL469), and *PPO2* (pLL467) were expressed in the *E. coli* BL21-AI strain at 37°C for 4–6 hr as insoluble His-tagged proteins. Inclusion bodies were purified from bacteria using the B-PER II Bacterial Protein Extraction Reagent (Pierce) according to the manufacturer's instructions. After separation of 300 μg of inclusion bodies on a single-slot SDS-PAGE, the gel band containing the recombinant protein was excised, homogenized, and injected into a rabbit for immunization. One month later, rabbits were challenged with three subsequent boosts of 150 μg of isolated inclusion bodies at intervals of 2 weeks and bled after each boost. A small volume of the final bleed serum for LRIM1 and APL1 was purified by an adapted small-scale affinity purification method (Smith and Fisher, 1984). For immunoblotting experiments, purified anti-LRIM1 and anti-APL1 antibodies were used at a dilution of 1/500. Anti-PPO2 serum was used at a dilution of 1/20,000.

Protein Purification and Limited Proteolysis

TEP1r-6×His was cloned, expressed, and purified as previously described (Baxter et al., 2007). Large-scale trypsinolysis of TEP1r-6×His was performed using bovine pancreatic trypsin (Sigma) at a 1:20 molar ratio to TEP1 in 0.2 M NaCl and 20 mM HEPES pH 7.5. Samples were incubated for 5 min at 37°C, then placed on ice and diluted 2-fold with 20 mM HEPES pH 7.5, 0.2 mM Leupeptin hemisulfate (Sigma), and 0.2 mM soybean trypsin-chymotrypsin inhibitor. Samples were immediately repurified on a Superdex 200 10/30 size exclusion column or Mono S 5/50 cation exchange column (GE Healthcare). Limited proteolysis on small scales was performed with trypsin, chymotrypsin, V8 protease, and elastase using similar buffer and incubation conditions but stopped by addition of 500 μM Pefabloc (Fluka; Buchs SG, Switzerland) followed directly by SDS-PAGE using Novex 4%–20% precast gels.

Thioester Assay

For each sample, two aliquots of 15 μl were mixed with 4 μl 5× Laemmli buffer without reducing agent. Following the addition of 1 μl 1 M DTT, the control sample (–) was incubated at room temperature for 15 min. The test sample (+) was placed at 94°C for 15 min, then cooled to room temperature prior to addition of 1 μl 1 M DTT. SDS-PAGE was performed using Novex 4%–20% precast gels.

Immunoprecipitation

One hundred fifty to two hundred female mosquitoes were anesthetized with CO_2 and injected with 69 nl of TEP1r-6×His (2.5 μg/μl in PBS) or with PBS alone using a Nanoject II Injector (Drummond). Mosquitoes were left for 3 hr and next homogenized in 1 ml IP buffer composed of Tris 50 mM pH 7.9, NaCl 100 mM, EDTA 2 mM, BSA 0.1 μg/ml, Tween 20 0.1%, and protease inhibitors (Complete Mini, Roche). Lipids and debris were removed by several rounds of centrifugation. For the following incubations, samples were kept at 4°C under constant shaking. For preclearance, extracts were incubated for 1 hr with 30 μl of Protein A-Sepharose beads slurry (GE Healthcare). Supernatant was next incubated for 1 hr with 1 μg anti-C-terminal 6×His-tag antibody (Invitrogen) and subsequently with 30 μl of Protein A-Sepharose slurry for another hour. Samples were centrifuged, and post-IP supernatant was collected. Sepharose beads were washed several times, alternating Tris-HCl 50 mM pH 7.9 Tween 20 0.1% and Tris-HCl 50 mM pH 7.9 Tween 20 0.1% NaCl 500 mM buffers. Antibodies and bound proteins were eluted from the beads in 40 μl protein loading buffer at 95°C for 3 min. Aliquots of post-IP supernatant and eluates were separated by 7% SDS-PAGE. Immunoblotting was performed as previously reported (Levashina et al., 2001).

SUPPLEMENTAL DATA

Supplemental Data include one figure and can be found online at http://www.cell.com/cellhostandmicrobe/supplemental/S1931-3128(09)00033-X.

ACKNOWLEDGMENTS

The authors thank J. Soichot, L. Huck, and M.E. Moritz for help with the mosquito colony and parasite cultures and Doctor E. Marois for fruitful discussions and critical reading of the manuscript. R.H.G.B. and Y.C. thank Professor J. Deisenhofer for continuing support. This work was supported by grants from the Centre National de la Recherche Scientifique (UPR 9022 du CNRS), the Institut National de la Recherche Medicale (AVENIR Inserm to E.A.L.), the French Ministry of National Education and Research (Allocation de Recherche to M.F. and S.S., AMN to C.F.), the Schlumberger Foundation for Education and Research (FSER, E.A.L.), EMBO Young Investigator Program (E.A.L.), EC FP6th Networks of Excellence "BioMalPar" (E.A.L. and J.A.H.), and the National Institutes of Health (2P01I44220-06A1 to J.A.H.). E.A.L. is an international research scholar of the Howard Hughes Medical Institute.

Received: July 15, 2008
Revised: October 31, 2008
Accepted: January 17, 2009
Published: March 18, 2009

REFERENCES

Baxter, R.H., Chang, C.I., Chelliah, Y., Blandin, S., Levashina, E.A., and Deisenhofer, J. (2007). Structural basis for conserved complement factor-like function in the antimalarial protein TEP1. Proc. Natl. Acad. Sci. USA *104*, 11615–11620.

Blandin, S., and Levashina, E.A. (2004). Thioester-containing proteins and insect immunity. Mol. Immunol. *40*, 903–908.

Blandin, S., Moita, L.F., Kocher, T., Wilm, M., Kafatos, F.C., and Levashina, E.A. (2002). Reverse genetics in the mosquito *Anopheles gambiae*: targeted disruption of the *Defensin* gene. EMBO Rep. *3*, 852–856.

Blandin, S., Shiao, S.H., Moita, L.F., Janse, C.J., Waters, A.P., Kafatos, F.C., and Levashina, E.A. (2004). Complement-like protein TEP1 is a determinant of vectorial capacity in the malaria vector *Anopheles gambiae*. Cell *116*, 661–670.

Blandin, S.A., Marois, E., and Levashina, E.A. (2008). Antimalarial responses in *Anopheles gambiae*: from a complement-like protein to a complement-like pathway. Cell Host Microbe *3*, 364–374.

Christophides, G.K., Zdobnov, E., Barillas-Mury, C., Birney, E., Blandin, S., Blass, C., Brey, P.T., Collins, F.H., Danielli, A., Dimopoulos, G., et al. (2002). Immunity-related genes and gene families in *Anopheles gambiae*. Science *298*, 159–165.

Collins, F.H., Sakai, R.K., Vernick, K.D., Paskewitz, S., Seeley, D.C., Miller, L.H., Collins, W.E., Campbell, C.C., and Gwadz, R.W. (1986). Genetic selection of a *Plasmodium*-refractory strain of the malaria vector *Anopheles gambiae*. Science *234*, 607–610.

de Marco, A. (2007). Protocol for preparing proteins with improved solubility by co-expressing with molecular chaperones in *Escherichia coli*. Nat. Protocols *2*, 2632–2639.

Dong, Y., Aguilar, R., Xi, Z., Warr, E., Mongin, E., and Dimopoulos, G. (2006). *Anopheles gambiae* immune responses to human and rodent *Plasmodium* parasite species. PLoS Pathog. *2*, e52.

Franke-Fayard, B., Trueman, H., Ramesar, J., Mendoza, J., van der Keur, M., van der Linden, R., Sinden, R.E., Waters, A.P., and Janse, C.J. (2004). A *Plasmodium berghei* reference line that constitutively expresses GFP at a high level throughout the complete life cycle. Mol. Biochem. Parasitol. *137*, 23–33.

Frolet, C., Thoma, M., Blandin, S., Hoffmann, J.A., and Levashina, E.A. (2006). Boosting NF-kappaB-dependent basal immunity of *Anopheles gambiae* aborts development of *Plasmodium berghei*. Immunity *25*, 677–685.

Gros, P., Milder, F.J., and Janssen, B.J. (2008). Complement driven by conformational changes. Nat. Rev. Immunol. *8*, 48–58.

Janse, C.J., and Waters, A.P. (1995). *Plasmodium berghei*: the application of cultivation and purification techniques to molecular studies of malaria parasites. Parasitol. Today *11*, 138–143.

Kobe, B., and Kajava, A.V. (2001). The leucine-rich repeat as a protein recognition motif. Curr. Opin. Struct. Biol. *11*, 725–732.

Lachmann, P.J., and Hughes-Jones, N.C. (1984). Initiation of complement activation. Springer Semin. Immunopathol *7*, 143–162.

Lambris, J.D., Reid, K.B., and Volanakis, J.E. (1999). The evolution, structure, biology and pathophysiology of complement. Immunol. Today *20*, 207–211.

Levashina, E.A., Moita, L.F., Blandin, S., Vriend, G., Lagueux, M., and Kafatos, F.C. (2001). Conserved role of a complement-like protein in phagocytosis revealed by dsRNA knockout in cultured cells of the mosquito, *Anopheles gambiae*. Cell *104*, 709–718.

Liszewski, M.K., Farries, T.C., Lublin, D.M., Rooney, I.A., and Atkinson, J.P. (1996). Control of the complement system. Adv. Immunol. *61*, 201–283.

Moita, L.F., Wang-Sattler, R., Michel, K., Zimmermann, T., Blandin, S., Levashina, E.A., and Kafatos, F.C. (2005). In vivo identification of novel regulators and conserved pathways of phagocytosis in *A. gambiae*. Immunity *23*, 65–73.

Niare, O., Markianos, K., Volz, J., Oduol, F., Toure, A., Bagayoko, M., Sangare, D., Traore, S.F., Wang, R., Blass, C., et al. (2002). Genetic loci affecting resistance to human malaria parasites in a West African mosquito vector population. Science *298*, 213–216.

Nurnberger, T., Brunner, F., Kemmerling, B., and Piater, L. (2004). Innate immunity in plants and animals: striking similarities and obvious differences. Immunol. Rev. *198*, 249–266.

Obbard, D.J., Callister, D.M., Jiggins, F.M., Soares, D.C., Yan, G., and Little, T.J. (2008). The evolution of *TEP1*, an exceptionally polymorphic immunity gene in *Anopheles gambiae*. BMC Evol. Biol. *8*, 274.

Osta, M.A., Christophides, G.K., and Kafatos, F.C. (2004). Effects of mosquito genes on *Plasmodium* development. Science *303*, 2030–2032.

Riehle, M.M., Markianos, K., Niare, O., Xu, J., Li, J., Toure, A.M., Podiougou, B., Oduol, F., Diawara, S., Diallo, M., et al. (2006). Natural malaria infection in *Anopheles gambiae* is regulated by a single genomic control region. Science *312*, 577–579.

Riehle, M.M., Markianos, K., Lambrechts, L., Xia, A., Sharakhov, I., Koella, J.C., and Vernick, K.D. (2007). A major genetic locus controlling natural *Plasmodium falciparum* infection is shared by East and West African *Anopheles gambiae*. Malar. J. *6*, 87.

Riehle, M.M., Xu, J., Lazzaro, B.P., Rottschaefer, S.M., Coulibaly, B., Sacko, M., Niare, O., Morlais, I., Traore, S.F., and Vernick, K.D. (2008). *Anopheles gambiae* APL1 is a family of variable LRR proteins required for Rel1-mediated protection from the malaria parasite, *Plasmodium berghei*. PLoS ONE *3*, e3672.

Sim, R.B., and Sim, E. (1981). Autolytic fragmentation of complement components C3 and C4 under denaturing conditions, a property shared with alpha 2-macroglobulin. Biochem. J. *193*, 129–141.

Sim, R.B., Twose, T.M., Paterson, D.S., and Sim, E. (1981). The covalent-binding reaction of complement component C3. Biochem. J. *193*, 115–127.

Sinden, R.E. (2002). Molecular interactions between *Plasmodium* and its insect vectors. Cell. Microbiol. *4*, 713–724.

Smith, D.E., and Fisher, P.A. (1984). Identification, developmental regulation, and response to heat shock of two antigenically related forms of a major nuclear envelope protein in *Drosophila* embryos: application of an improved method for affinity purification of antibodies using polypeptides immobilized on nitrocellulose blots. J. Cell Biol. *99*, 20–28.

Whitten, M.M., Shiao, S.H., and Levashina, E.A. (2006). Mosquito midguts and malaria: cell biology, compartmentalization and immunology. Parasite Immunol. *28*, 121–130.